INTERNATIONAL SOCIETY FOR SOIL MECHANICS AND GEOTECHNICAL ENGINEERING

The paper was published in the proceedings of the 12th Australia New Zealand Conference on Geomechanics and was edited by Graham Ramsey. The conference was held in Wellington, New Zealand, 22-25 February 2015.

Deformation behaviour of coal-fouled ballast reinforced with geogrid

N. T. Ngo[1], C. Rujikiatkamjorn[2] and B. Indraratna[3], FTSE, FIEAust, FASCE.

[1]Centre for Geomechanics and Railway Engineering; ARC Centre for Excellence for Geotechnical Science and Engineering, Faculty of Engineering and Information Sciences, University of Wollongong, NSW 2522, Australia; PH (+61) 4221-4892; email: trung@uow.edu.au
[2]Centre for Geomechanics and Railway Engineering; ARC Centre for Excellence for Geotechnical Science and Engineering, Faculty of Engineering and Information Sciences, University of Wollongong, NSW 2522, Australia; PH (+61) 4221-5852; email: cholacha@uow.edu.au
[3]Research Director, Professor of Civil Engineering, Centre for Geomechanics and Railway Engineering; ARC Centre for Excellence for Geotechnical Science and Engineering, Faculty of Engineering and Information Sciences, University of Wollongong, NSW 2522, Australia; PH (+61) 4221-3046; FAX (+61) 4221-3238; email: indra@uow.edu.au

ABSTRACT

This paper presents the results of an experimental study of coal-fouled ballast reinforced with geogrid, at various degrees of fouling and subjected to cyclic loading. A novel Track Process Simulation Testing Apparatus was used to realistically simulate fouled rail track conditions. The laboratory results demonstrated that coal fines acted as a lubricant, causing ballast aggregates to displace and rotate, and as a result, increase the deformation of ballast. However, coal fines also reduced ballast breakage somewhat because they fill the voids between the ballast particles and coat surface of ballast aggregates which reduce the inter-particle attrition. The placement of a geogrid at the interface between the ballast and sub-ballast layers provides extra internal confinement and interlocks the grains of ballast in its apertures, which also reduces ballast deformation. Based on laboratory results, a threshold value of VCI=40% is proposed to assist practitioners in conducting track maintenance as if fouling beyond this threshold significantly reduces the reinforcement effect of geogrid such that fouled ballast experiences premature dilation leading to track instability. A novel equation incorporating the Void Contaminant Index and number of load cycles is also introduced to predict the deformation of fouled ballast, improve the design of rail tracks, and help make the correct decisions with regards to track maintenance.

Keywords: ballast, fouling, coal fines, geogrid, cyclic loading

INTRODUCTION

Ballast is a free draining granular material used as a load bearing platform in railway tracks to transmit and distribute the wheel load to the underlying sub-ballast and subgrade at a reduced stress level (Selig and Waters 1994). During track operations, ballast progressively deteriorates and becomes fouled due to breakage and the infiltration of external fine particles (e.g., clay, coal fines). Fouling has traditionally been considered as an unfavourable condition for the track structure (Indraratna et al. 2011). In a given typical Australian coal freight tracks, Feldman and Nissen (2002) presented that dry coal fines constitute 70-95% of the fouling materials in ballasted rail tracks. Budiono et al. (2004) stated that coal fines adversely affect the deformation and shear strength of the track. Dombrow et al. (2009) and Huang et al. (2009) conducted direct shear tests for fouled ballast at different levels of fouling and showed that the shear strength steadily decreases with an increased level of fouling.

Geogrids have been widely used to stabilise ballast and increase the duration of track serviceability because it provides additional internal confining pressure (Bathurst and Raymond 1987; Raymond 2002; Brown et al. 2006; Fernandes et al. 2008; Indraratna et al. 2011; Ngo et al. 2014). The ability of geogrid to constrain railway ballast comes through the non-horizontal displacement boundary that restrains the ballast by interlocking between itself and the ballast grains.

When ballast is fouled by breakage or the infiltration of fine particles, the interaction between the geogrid and ballast grains may change considerably as fine particles accumulate within the ballast voids and reduce the mechanical interlocking and friction between the geogrid and ballast (Indraratna et al. 2014). There have only been limited studies conducted for coal-fouled ballast reinforced by geogrid. Indraratna et al. (2011) conducted series of large-scale direct shear tests to investigate how the interface between ballast and geogrid copes with coal fouling, but this study does not represent actual field condition where the composite ballast-geogrid system is subjected to cyclic train loadings at low confining pressures. This paper presents a study of the deformation of coal-fouled ballast reinforced with geogrid subjected to cyclic loading.

MATERIAL TESTED

Samples of ballast were collected from Bombo quarry, New South Wales, Australia, and then cleaned and sieved according to the Australian Standard (AS 2758.7, 1996). In Australia, the vast majority of coal lines are mainly fouled by coal falling off the wagons during the passage of coal freight trains. Dry coal fines were provided by Queensland Rail and used as fouling material in this study, and the Void Contamination Index (VCI) introduced earlier by Indraratna et al. (2010) was adopted to quantify ballast fouling. The advantage of VCI is that it considers different fouling material by incorporating their respective specific gravities, as given below:

$$VCI = \frac{1+e_f}{e_b} \times \frac{G_{sb}}{G_{sf}} \times \frac{M_f}{M_b} \times 100 \qquad (1)$$

where e_f= void ratio of fouling material, e_b= the void ratio of fresh ballast, G_{sb}= the specific gravity of ballast, G_{sf}= the specific gravity of fouling material, M_f= the dry mass of fouling material, M_b= the dry mass of fresh ballast.

The particle size distributions of ballast and coal fines adopted in this study are shown in Figure 1. The grain size characteristics of the ballast and sub-ballast, and the engineering properties of coal fines used in this study are presented in Table 1 and Table 2, respectively. Polypropylene bi-axial geogrid with 40 mm x 40 mm size apertures was provided by Polyfabric Australia Pty Ltd. The tensile strength of the geogrid is 30 kN/m. It is commonly used in Australian railway tracks and was adopted in this study.

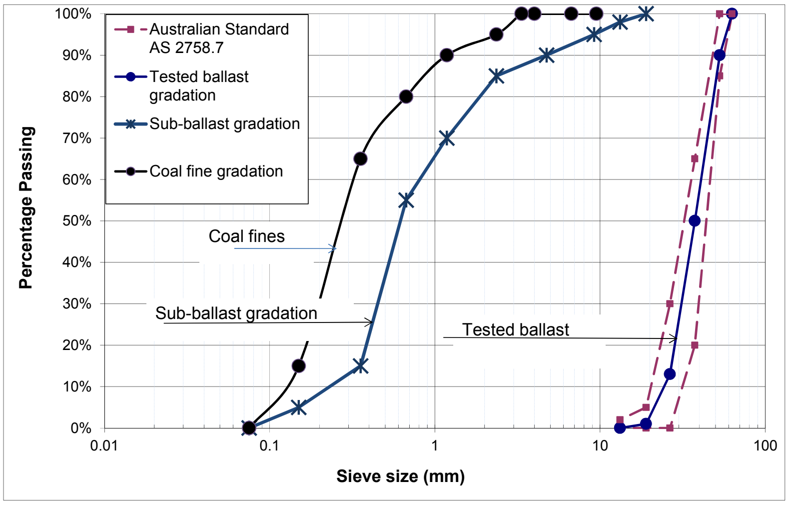

Figure 1. Particle size distributions of ballast sub-ballast and coal fines

Table 1. Grain size characteristics of ballast and sub-ballast

Material	Particle shape	d_{max} (mm)	d_{10} (mm)	d_{30} (mm)	d_{50} (mm)	d_{60} (mm)	C_u	C_c	Size ratio
Ballast	Highly angular	53	16	28	35	39	2.4	1.3	11.3
Sub-ballast	Angular to rounded	19	0.23	0.45	0.61	0.8	3.5	1.1	31.6

Note: d_{max} : maximum size ballast used in this study; d_{10}: diameter in millimetres at which 10% by weight of ballast passes through the sieve; d_{30}, d_{50}, d_{60}: diameters in millimetres at which 30% , 50%, and 60% by weight of ballast passes through the sieve; C_u: coefficient of uniform, defined by: $C_u=d_{60}/d_{10}$; C_c: coefficient of curvature, defined by: $C_c=(d_{30})^2/d_{10}/ d_{60}$; Size ratio: ratio of apparatus dimension divided by maximum particle size;

Table 2. Engineering properties of coal fines

	Specific gravity	Liquid limit (%)	Plastic limit (%)	Optimum moisture content, OMC (%)	Maximum dry density (kg/m^3)	Mean particle size d_{50} (mm)
Coal fines	1.28	91	50	35	874	0.28

TRACK PROCESS SIMULATION APPARATUS

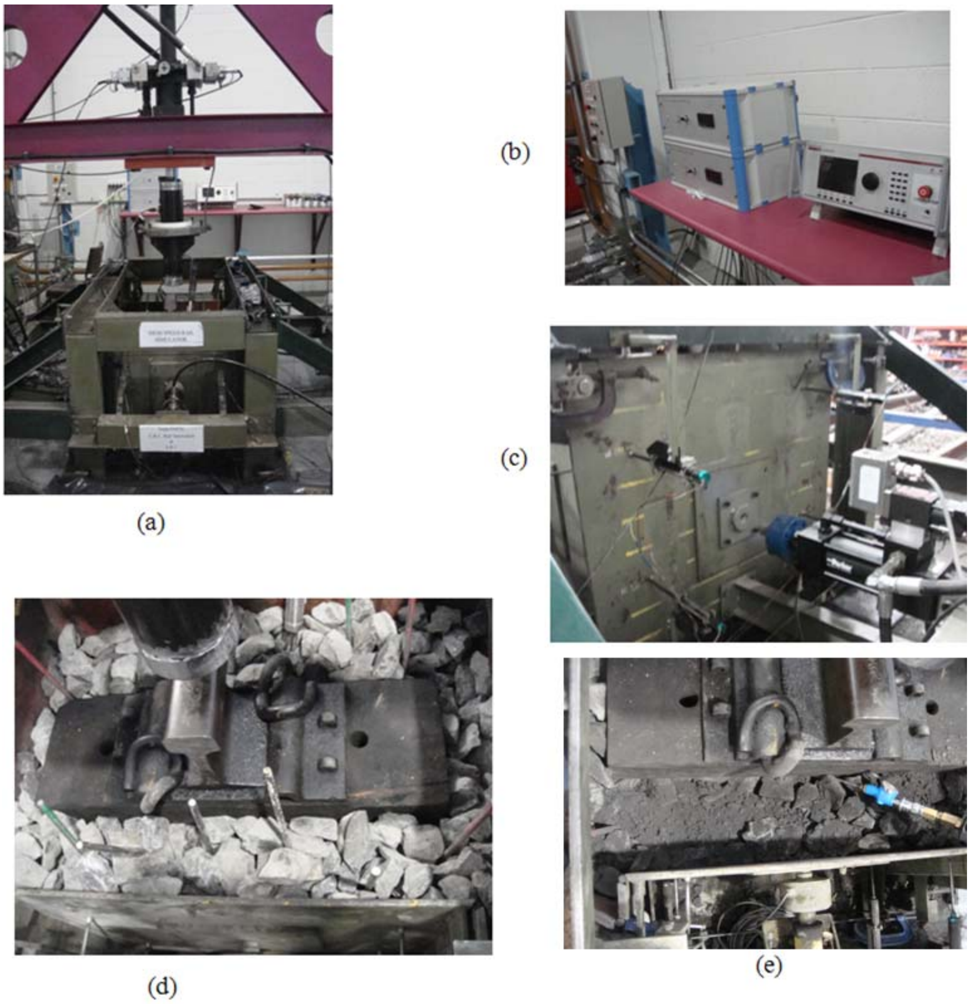

Figure 2. Primary components of TPSA: (a) general view of the equipment; (b) confining pressure control unit; (c) hydraulic jack, potentiometers and clamps; (d) placement of sleeper on ballast layer; (e) spreading coal fines

A novel Rail Process Simulation Testing Apparatus (TPSA) was modified based on an original design by Indraratna and Salim (2003). It has four main parts: a prismoidal triaxial tank, an axial loading system, a confining pressure control unit, and horizontal and vertical displacement recording equipment. The general view and typical components of the TPSA are shown in Figure 2. The TPSA can simulate a ballast assembly 800-mm long x 600-mm wide x 600-mm high. A system of hinges and ball bearings was lubricated to allow the vertical walls to move horizontally with minimum friction. Steel pegs were placed at each of the sleeper/ballast and ballast/sub-ballast interfaces to capture settlement of the ballast layer. Cyclic loading was generated by a servo hydraulic actuator and applied through the ballast via a wooden sleeper connected to a steel rail. The lateral confining pressures applied in two horizontal directions (perpendicular and parallel to the sleeper) were generated by hydraulic jacks, to which load cells were connected, as shown in Figure 2c. The applied confining pressures were selected based on the lateral confinement provided by the weight of crib and shoulder ballast, along with particle frictional interlock Typically, for NSW ballast gradations, the initial stresses were kept constant around 6-7 kPa in the transverse direction (parallel to sleeper), and about 10-12 kPa along the longitudinal direction for which the lateral strains have to be kept as small as possible. The applied confining pressures adopted in this study are justified by field measurements from Singleton and Bulli tracks in NSW. Horizontal displacement of the vertical walls was recorded using 16 electronic potentiometers. All the tests were carried out at a frequency of 15 Hz with a maximum applied cyclic stress of 420 kPa (Figure 3), and subjected to up to 500,000 load cycles. The frequency and cyclic loading were determined for freight trains travelling at close to 90 km/h in Australia (Indraratna et al. 2011). Every instrument was calibrated before being connected to an electronic DT800 data logger that was controlled by a host computer supported by Labview software to accurately record settlement, pressures, and horizontal movement of the associated walls at pre-determined time intervals.

EXPERIMENTAL PROGRAM

A total of 10 tests were carried out for coal-fouled ballast with and without the inclusion of geogrid, and with a VCI between 0% and 70%. The experimental program and weight of materials used for each test are shown in Table 1. All the side walls of the TPSA were fastened to prevent any displacement while the ballast sample was being compacted. Layers of subgrade and sub-ballast were prepared to the desired unit weights using a vibratory compactor, as mentioned previously. A pressure plate, settlement pegs, and geogrid were then placed onto the layer of sub-ballast. The ballast was placed in the TPSA and compacted into five layers by a vibratory compactor to a dry density of 1530kg/m^3. A rubber pad was placed beneath the vibrator to prevent particle breakage during compaction. To simulate fouling, a predetermined amount of coal fines were sprayed over each layer to meet the desired VCI. These coal fines then migrated and accumulated into voids between the particles of ballast under gravity and vibration. The remaining ballast was then added until the ballast attained its final height of 300 mm and was then compacted further to achieve the desired unit dry bulk density. A wooden sleeper was then placed on top of the ballast and connected to a hydraulic actuator via a steel ram. Eight settlement pegs were placed on top of the ballast, and then more ballast was placed onto the top level of the sleeper to represent the crib and shoulder ballast.

Table 1. Experimental program and weight of materials used in each test

VCI (%)	Without geogrid	With biaxial geogrid 40 mm x 40 mm	Weight of ballast (kg)	Weight of coal fines (kg)
0	X	X	220	0
10	X	X	220	5.20
20	X	X	220	10.40
40	X	X	220	20.80
70	X	X	220	36.40

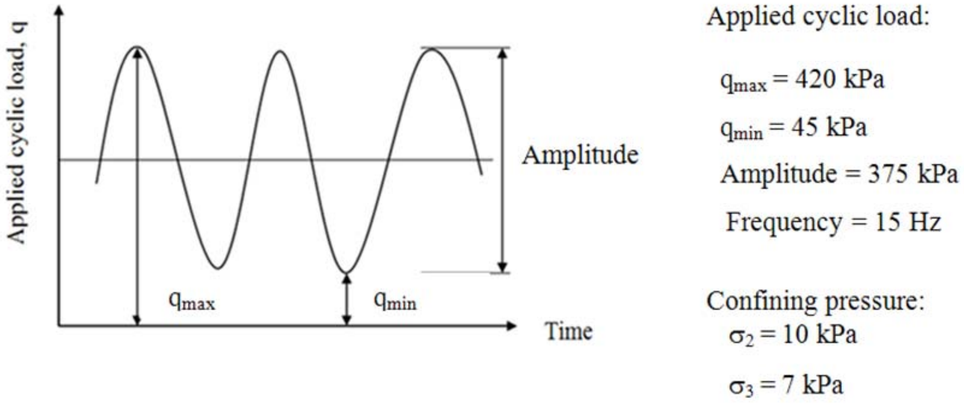

Figure 3. Typical cyclic loading applied in the study

After the ballast sample was prepared, the clamps were removed and lateral pressures (σ_2=10 kPa and σ_3=7 kPa) corresponding to confining pressures typically provided by crib and shoulder ballast in the real track were applied (Figure 2c). An initial vertical stress of 45 kPa was then applied to the sleeper to stabilise the ballast assembly and act as a reference for all horizontal movement and settlement recordings. A cyclic load was then applied through a servo hydraulic actuator to simulate the loading pattern shown in Figure 3. This loading pattern generated an approximately average pressure of 233 kPa onto the sleeper and ballast interface, which represented a 20 tonne/axle train running at around 90 km/h under typical Australian track conditions. A total of 500,000 load cycles was simulated in every test, but this was stopped at predetermined cycles to take readings of the settlement pegs and capture the resilience of ballast at the end of these cycles. Horizontal displacements and vertical stresses were automatically recorded by an automated DT800 data logger.

RESULTS AND DISCUSSION

Deformation of Coal-fouled Ballast

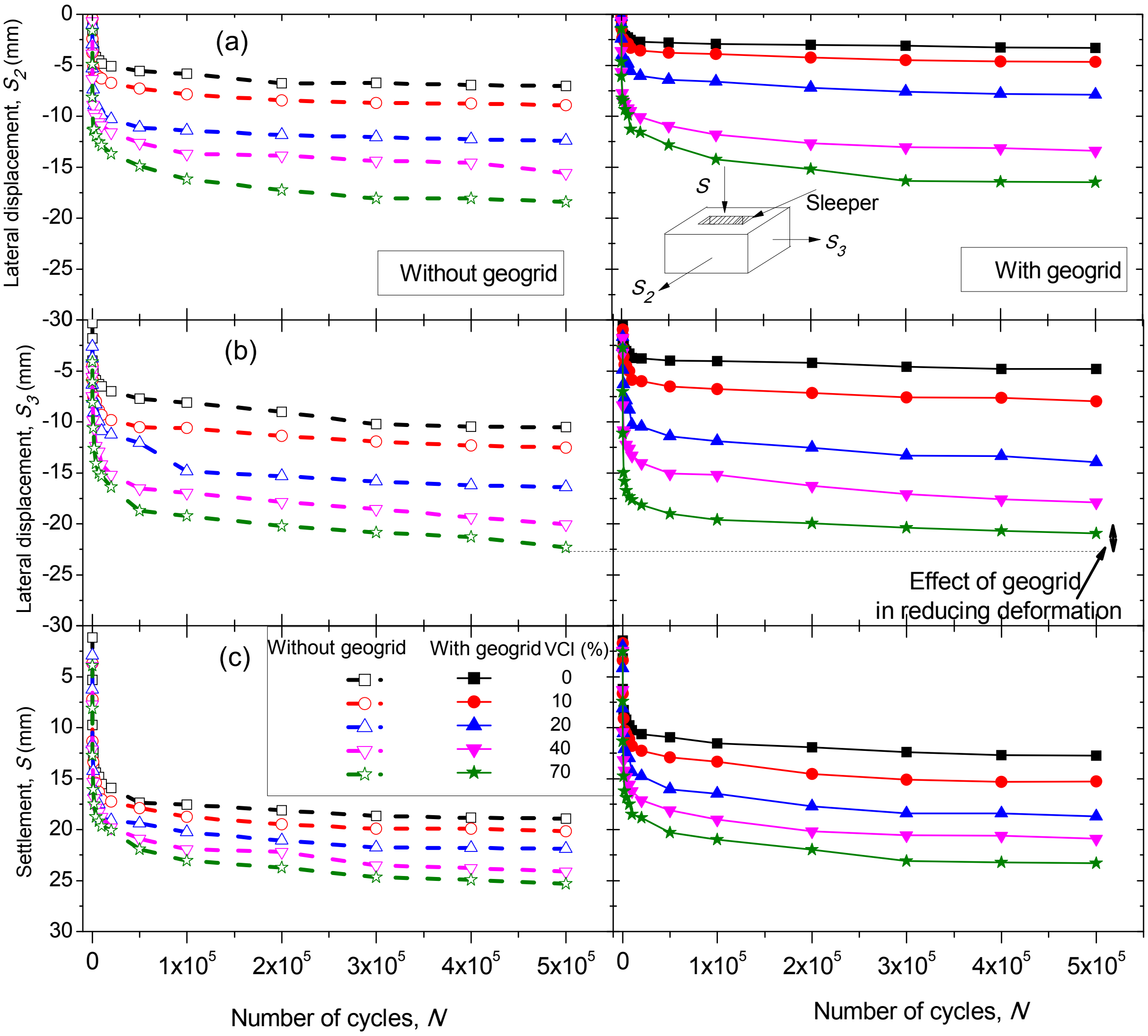

Figure 4. Deformation of coal-fouled ballast with and without geogrid at varying VCIs: (a) lateral displacement (perpendicular to sleeper); (b) lateral displacement (parallel to sleeper); (c) vertical settlement (modified after Indraratna et al. 2013)

Figure 4a and 4b show the lateral displacement and vertical settlement of coal-fouled ballast with and without geogrid reinforcement. It can be seen that the geogrid decreased the lateral displacement of fresh and fouled ballast quite considerably because the ballast created a strong mechanical interlock with the geogrid due to interlocking. This interlocking effect enabled the geogrid to act as a fixed boundary which reduced deformation. This is in good agreement with previous studies conducted by McDowell et al. (2006), where the discrete element method (DEM) was adopted to study the interaction between geogrid and ballast. They reported that the geogrid acts like an efficient interlock by forming a stiffened zone inside the ballast assembly. An increased VCI leads to a remarkably higher horizontal displacement and larger settlement. Indeed, when fouling increases, the coal fines would act as a lubricant which assists the particles to slide and/or roll over each other, which in turn, would increase deformation. However, the ability of geogrid to decrease ballast deformation also reduces when the VCI increases because at the end of every test, coal fines had accumulated in the apertures of the geogrids which decreased the effective size of the geogrid aperture.

The settlement of fouled ballast with and without the inclusion of geogrid at various VCIs is also presented in Figure 4c. It was observed that the geogrid-reinforced ballast exhibited less settlement than the unreinforced ballast assembly for any given VCI. All the samples experienced an identical initial rapid settlement up to 100,000 cycles, followed by gradually increasing settlement within 300,000 cycles, and then remained relatively stable thereafter. This was mainly because ballast undergoes significant rearrangement and densification within the initial loading cycles, but after achieving a threshold compression, any further loading would withstand subsequent settlement. It was also noted that a larger VCI-fouled sample of ballast exhibited a higher settlement. This increased settlement is associated with coal fines which would act as a lubricant assisting the ballast grains to slide and/or roll over each other, which in turn, would increase settlement.

The observed data are best presented by Figure 5, which shows the final values of deformation and the relatively deformation factor at N=500,000 with varying VCIs. The relatively deformation factor (R) can be described as follows:

Vertical settlement (%) : $$R_s = \frac{S_{(\mathrm{unreinforced})} - S_{(\mathrm{reinforced})}}{S_{(\mathrm{unreinforced})}} \times 100 \qquad (2)$$

Lateral deformation (%): $$R_{h2} = \frac{S_{2(\mathrm{unreinforced})} - S_{2(\mathrm{reinforced})}}{S_{2(\mathrm{unreinforced})}} \times 100 \qquad (3)$$

Lateral deformation (%): $$R_{h3} = \frac{S_{3(\mathrm{unreinforced})} - S_{3(\mathrm{reinforced})}}{S_{3(\mathrm{unreinforced})}} \times 100 \qquad (4)$$

The ability of geogrid to reduce the deformation of ballast is elucidated by the values of R shown in Figure 5. The benefit of geogrid became marginal if the VCI went beyond 40%. Indeed, the geogrid performed best when placed in a fresh ballast assembly (approximately 52% and 32% reduction for lateral and vertical deformation, respectively), but it's performed decreased significantly with an increase of VCI (approximately 5% and 12% reduction for lateral and vertical deformation for VCI=40%). This result was justified by the fact that where VCI=40% or beyond, coal fines coat the ballast grains and clog the openings of the geogrid, preventing inter-particle friction mobilisation and effectively interlocking with the geogrid. Based on this observation, it is possible to propose a threshold value of VCI=40%, where the benefits of geogrid become marginal and track maintenance is needed.

Based on the data measured experimentally, this study is a first attempt to propose an empirical equation to predict track settlement, (S) considering the degree of fouling, (VCI) as defined by:

$$S = a + \frac{b}{1-\mathrm{VCI}} \log_{10} N \qquad (5)$$

Where, S is the settlement, VCI is the Void Contaminant Index $(0 \le \mathrm{VCI} < 1)$, a and b are empirical coefficients depending on VCI, and N is the number of load cycles.

A comparison of ballast settlement with and without geogrid at varying VCI, compared to the results based on Equation (5), is presented in Figure 6. The calculated settlements match with data measured from laboratory. The empirical values a and b at differrent VCIs were also given in Figure 6 which are applicable for test set up condition and the common ballast type (latite basalt) and the coal fouling material in Australian freight tracks. From a practical perspective, the proposed Equation 7 can help practicing engineers predict track settlement and simultaneously consider ballast fouling

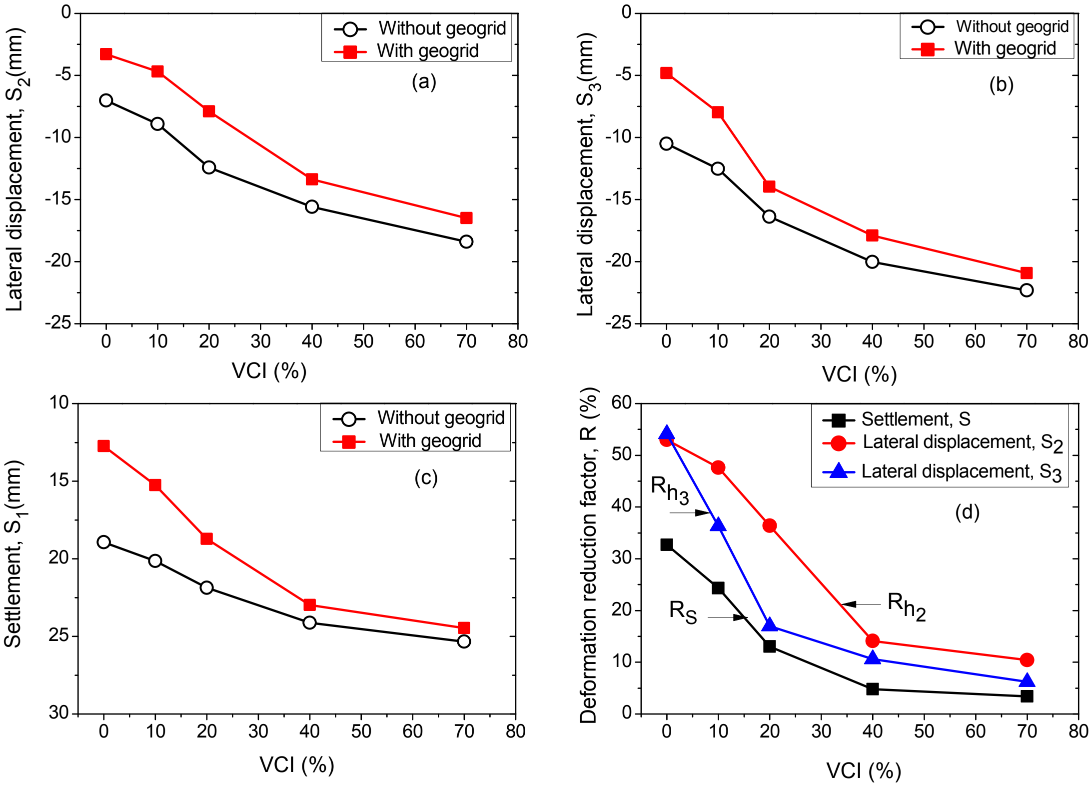

Figure 5. Variations of final deformation of fresh and fouled ballast with and without geogrid, with VCI: (a) lateral displacement S2; (b) lateral displacement S3; (c) settlement S; (d) ballast deformation factor, R (modified after Indraratna et al. 2013)

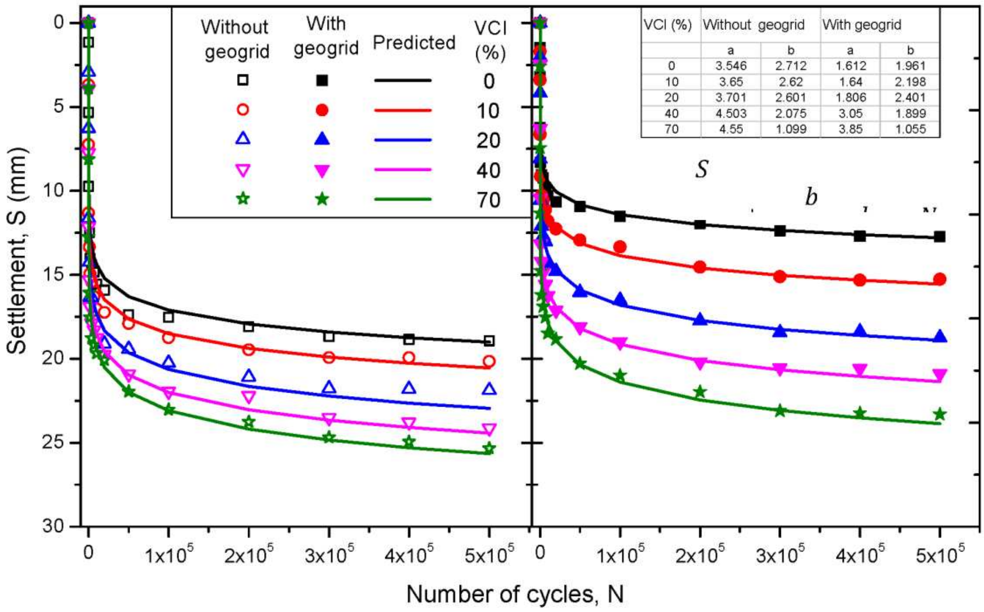

VCI (%)	Without geogrid		With geogrid	
	a	b	a	b
0	3.546	2.712	1.612	1.961
10	3.65	2.62	1.64	2.198
20	3.701	2.601	1.806	2.401
40	4.503	2.075	3.05	1.899
70	4.55	1.099	3.85	1.055

Figure 6. Comparisons of ballast settlement at varying VCI with/without geogrid inclusion measured experimentally and predicted (modified after Indraratna et al. 2013)

CONCLUSIONS

Ten tests of fresh and coal-fouled ballast at different VCIs with and without geogrid were carried out to investigate the deformation behaviour of ballast using a novel TPSA. The TPSA was used to simulate more realistic Australian track conditions. The results show that all the ballast samples experienced a considerable amount of deformation within 100,000 cycles, followed by a gradual increase in settlement up to 300,000 cycles, and then remained relatively stable. The study found that while the geogrid decreased deformation due to the interlocking effect, coal fines increased deformation because of the lubricant effect. Geogrid provides the most benefit in terms of reducing deformation with fresh ballast (providing about 52% and 32% reduction for lateral and vertical deformation, respectively), but this effect decreased with an increase of VCI (providing about 5% and 12% reduction for lateral and vertical deformation where VCI=40%). Based on this study, it is possible to propose a threshold value of VCI=40%, where the benefit of geogrid becomes marginal and track maintenance is required. A novel equation was proposed to predict ballast settlement while considering the level of fouling.

ACKNOWLEDGEMENTS

The Authors acknowledge the financial support provided by Australian Research Council, Cooperative Research Centre for Rail Innovation, and support from the Centre for Geomechanics and Railway Engineering, University of Wollongong, NSW, Australia. A significant portion of these contents were reproduced with kind permission from the Journal of Geotechnical and Geoenvironmental Engineering, ASCE.

REFERENCES

Bathurst, R.J, and Raymond, G.P. (1987). “Geogrid reinforcement of ballasted track”, Transportation Research Record, 1153, 8-14.

Brown, S.F., Thom, N.H., and Kwan, J. (2006). “Optimising the geogrid reinforcement of rail track ballast”, Railfound Conference, Birmingham.

Budiono, D. S., McSweeney, T., Dhanasekar, M., and Gurung, N. (2004). “The effect of coal dust fouling on the cyclic behaviour of railtrack ballast”, Cyclic Behaviour of Soils and Liquefaction phenomena, Taylor & Francis Group, London.

Dombrow, W., Huang, H., and Tutumluer, E. (2009). “Comparison of coal dust fouled railroad ballast behavior-granite vs. limestone”, Bearing Capacity of Roads, Railways and Airfields, Proceedings of the 8th International Conference (BCR2A'09), Taylor & Francis Group.

Fernandes, G., Palmeira, E.M., and Gomes, R.C. (2008). “Performance of geosynthetic-reinforced alternative sub-ballast material in a railway track”, Geosynthetics International, 15(5), 311-321.

Feldman, F., and Nissen, D. (2002). “Alternative testing method for the measurement of ballast fouling”, Conference on Railway Engineering, Wollongong: RTSA.

Huang, H., Tutumluer, E., and Dombrow, W. (2009). “Laboratory characterisation of fouled railroad ballast behaviour”, Transportation Research Record: Journal of the ransportation Research Board, No. 2117. Washington, DC.

Indraratna, B., and Salim, W. (2003). “Deformation and degradation mechanics of recycled ballast stabilised with geosynthetics”, Soils and Foundations, 43(4), 35-46.

Indraratna, B., Nimbalkar, S., and Tennakoon, N. (2010). “The Behaviour of Ballasted Track Foundations: Track Drainage and Geosynthetic Reinforcement”, GeoFlorida, Advances in Analysis, Modeling & Design (GSP 199), 2378-2387.

Indraratna, B., Ngo, N.T., and Rujikiatkamjorn, C. (2011). “Behavior of geogrid-reinforced ballast under various levels of fouling”, Geotextiles and Geomembranes, 29(3): p. 313-322.

Indraratna, B., Salim, W., and Rujikiatkamjorn, C. (2011). “Advanced rail geotechnology - ballasted track”, CRC Press, Taylor & Francis Group, London, UK.

Indraratna, B., Ngo, N.T., and Rujikiatkamjorn, C. (2013). “Deformation of Coal Fouled Ballast Stabilized with Geogrid under Cyclic Load”, Journal of Geotechnical and Geoenvironmental Engineering, 139(8), 1275-1289.

Indraratna, B., Ngo, N.T, Rujikiatkamjorn, C., and Vinod, J.(2014) “Behaviour of Fresh and Fouled Railway Ballast subjected to Direct Shear Testing - A Discrete Element Simulation”, International Journal of Geomechanics, ASCE, 14(1), 34-44.

McDowell, G.R., Harireche, O., Konietzky, H., Brown, S. F., and Thom, N. H.(2006). “Discrete element modelling of geogrid-reinforced aggregates”, Proceedings of the ICE - Geotechnical Engineering. 159(1), 35-48.

Ngo, N.T., Indraratna, B., and Rujikiatkamjorn, C. (2014). “DEM simulation of the behaviour of geogrid stabilised ballast fouled with coal”, Computers and Geotechnics, 55, 224-231.

Raymond, G.P. (2002). “Reinforced ballast behaviour subjected to repeated load”, Geotextiles and Geomembranes, 20(1), 39-61.

Selig, E.T. and Waters, J.M. (1994) “Track geotechnology and substructure management”, Thomas Telford, London.